Extracting Higher Central Charge from a Single Wave Function

Ryohei Kobayashi,^{1,*} Taige Wang®,^{2,3} Tomohiro Soejima (副島智大),²
Roger S. K. Mong (蒙紹璣),⁴ and Shinsei Ryu®⁵

¹Department of Physics, Condensed Matter Theory Center, and Joint Quantum Institute, University of Maryland,
College Park, Maryland 20742, USA

²Department of Physics, University of California, Berkeley, California 94720, USA

³Material Science Division, Lawrence Berkeley National Laboratory, Berkeley, California 94720, USA
⁴Department of Physics and Astronomy, University of Pittsburgh, Pittsburgh, Pennsylvania 15260, USA
⁵Department of Physics, Princeton University, Princeton, New Jersey 08544, USA



(Received 25 March 2023; revised 7 October 2023; accepted 18 November 2023; published 4 January 2024)

A (2+1)D topologically ordered phase may or may not have a gappable edge, even if its chiral central charge c_- is vanishing. Recently, it was discovered that a quantity regarded as a "higher" version of chiral central charge gives a further obstruction beyond c_- to gapping out the edge. In this Letter, we show that the higher central charges can be characterized by the expectation value of the partial rotation operator acting on the wave function of the topologically ordered state. This allows us to extract the higher central charge from a single wave function, which can be evaluated on a quantum computer. Our characterization of the higher central charge is analytically derived from the modular properties of edge conformal field theory, as well as the numerical results with the $\nu=1/2$ bosonic Laughlin state and the non-Abelian gapped phase of the Kitaev honeycomb model, which corresponds to $U(1)_2$ and Ising topological order, respectively. The Letter establishes a numerical method to obtain a set of obstructions to the gappable edge of (2+1)D bosonic topological order beyond c_- , which enables us to completely determine if a (2+1)D bosonic Abelian topological order has a gappable edge or not. We also point out that the expectation values of the partial rotation on a single wave function put a constraint on the low-energy spectrum of the bulk-boundary system of (2+1)D bosonic topological order, reminiscent of the Lieb-Schultz-Mattis-type theorems.

DOI: 10.1103/PhysRevLett.132.016602

Introduction.—(2+1)D topological phases with bulk energy gap host various intriguing physical phenomena [1]. One of the most striking is the bulk-edge correspondence, where the property of the bulk heavily constrains dynamics at its boundary. The most celebrated example is the integer quantum Hall effect, where the nonzero bulk Chern number implies the presence of gapless charged edge modes [2]. Even without charge conservation, systems with nonzero chiral central charge c_- , which signals nonzero thermal Hall conductance, has gapless edge modes [3]. We have a good theoretical understanding of these quantities through coarse-grained Chern-Simons theory, and we can extract them from microscopic wave functions [4–13].

In the presence of anyonic excitations, there are properties beyond c_{-} that enforce the presence of gapless edge modes. In many cases, nontrivial braiding statistics between anyons can present an obstruction to gapping out all anyonic degrees of freedom simultaneously at the boundary [14,15]. Such phases of matter are said to have an ungappable edge. Recently, it was discovered that a quantity called "higher central charge" can partially capture the "ungappability" of the edge [16,17]. In particular, higher central charges of an Abelian topological order completely determine whether it has an ungappable edge [18]. However, so far, the quantity

has been characterized purely through the topological quantum field theory (TQFT) framework, and a microscopic understanding of higher central charges has been lacking.

In this Letter, we show that the expectation value of the "partial rotation" operator—the rotation operator that acts only on a part of the system—can be used to reliably extract higher central charges of topologically ordered systems. This is the first proposal that relates the wave function of a topological ordered state to its higher central charges, and our operational definition even allows its evaluation on a quantum computer. Our finding is supported by an analytical conformal field theory (CFT) calculation, as well as numerics on the non-Abelian phase of the Kitaev honeycomb model and $\nu = 1/2$ bosonic Laughlin state. This Letter establishes a general numerical method to obtain obstructions to a gappable edge of a bosonic topological order beyond c_{-} , which enables us to completely determine if bosonic Abelian topological order has a gappable edge.

Definition and properties of higher central charge.— The higher central charges ζ_n are complex numbers characterizing a topologically ordered state, labeled by a positive integer n. ζ_n can be easily computed from the properties of anyons in the topological order; for a given bosonic (2+1)D topological order, ζ_n is defined as the following phase:

$$\zeta_n = \frac{\sum_a d_a^2 \theta_a^n}{|\sum_a d_a^2 \theta_a^n|},\tag{1}$$

where the sum is over all anyons in the topological order, d_a is quantum dimension, and θ_a is topological twist of an anyon a. When $n=1,\zeta_1$ reduces to the Gauss sum formula for chiral central charge modulo $8,\zeta_1=e^{(2\pi i/8)c_-}$, hence ζ_n formally provides a generalization of c_- .

Higher central charges put a constraint on the gappability of the edge; it was proven in [16] that $\zeta_n=1$ for all n such that $\gcd(n,N_{\text{FS}})=1$ give necessary conditions for a gappable edge. Here, N_{FS} is called the Frobenius-Schur exponent, defined as the smallest positive integer satisfying $\theta_a^{N_{\text{FS}}}=1$ for all anyons a. For example, $\operatorname{U}(1)_2\times\operatorname{U}(1)_{-4}$ Chern-Simons theory has $\zeta_3=-1$, which shows that the topological order has an ungappable edge even though $c_-=0$. For $(2+1)\mathrm{D}$ bosonic Abelian topological phases, one can also derive sufficient conditions: the higher central charges $\{\zeta_n\}$ for $\gcd\{n,[N_{\text{FS}}/\gcd(n,N_{\text{FS}})]\}=1$ give both necessary and sufficient conditions for a gappable boundary [18].

Main result.—To extract higher central charges from a single wave function, we consider a (2+1)D topological ordered state located on a cylinder. The state on the cylinder is labeled by the anyon a, which corresponds to a quasiparticle obtained by shrinking the puncture at the end of the cylinder. Suppose we have realized a ground state $|\Psi\rangle$ on the cylinder labeled by the trivial anyon 1. Let us take a bipartition of the cylinder into the two subsystems labeled by A and B and write the translation operator for the A subsystem by the angle θ along the circumference as $T_{A;\theta}$ (see Fig. 1). We then find that the following quantity extracts ζ_n :

$$\mathcal{T}_1\left(\frac{2\pi}{n}\right) := \langle \Psi | T_{\mathbf{A}; \frac{2\pi}{n}} | \Psi \rangle \propto e^{-2\pi i (\frac{2}{n} + n) \frac{c_-}{24}} \times \sum_a d_a^2 \theta_a^n, \quad (2)$$

where α in this Letter always means being proportional up to a positive real number. In the special case where n=1, the rhs becomes 1 since $\sum_a d_a^2 \theta_a \propto e^{(2\pi i/8)c_-}$, consistent with the fact that the 2π rotation of the cylinder A gives the identity. For n>1 and $\gcd(n,N_{\rm FS})=1$, the above rhs becomes proportional to ζ_n and gives a nontrivial obstruction to gapped boundary beyond c_- . Since c_- can be extracted from a single wave function [6,7], our method allows a complete characterization of all higher central charges.

For (2+1)D bosonic Abelian topological order, one can show that partial rotation, together with topological entanglement entropy [19,20], fully determines if its edge is gappable. See the Supplemental Material [21] for an explicit algorithm determining gappability. We also note

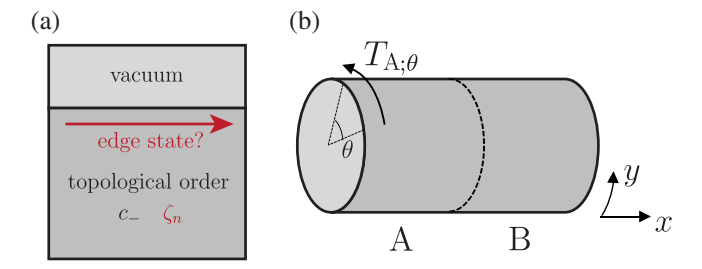


FIG. 1. (a) The setup for which we considered the gappability problem. The obstruction can be captured by c_{-} and higher central charge ζ_{n} . (b) Schematics of the partial rotation of a cylinder bisected into A and B subsystems.

that partial rotation, which is unitary, can be easily evaluated on a quantum computer using methods such as the Hadamard test.

Analytic derivation.—Equation (2) can be derived by employing the cut-and-glue approach established in [19,27], which describes the entanglement spectrum of the A subsystem at long wavelength by that of the (1+1)D CFT on its edges [28]. Namely, the reduced density matrix for the A subsystem is effectively given by $\rho_A = \rho_{A;l} \otimes \rho_{A;r}$, where $\rho_{A;l}, \rho_{A;r}$ denote the CFTs on the left and right edges, respectively. The left edge lies at the end of the whole cylinder realizing the ground state of CFT; the right edge of the A subsystem entangled with the B subsystem is described by a thermal density matrix of a perturbed edge CFT [29]. The form of the perturbation in the entanglement Hamiltonian is not universal. In the following, we assume that the entanglement Hamiltonian is that of the unperturbed CFT $\rho_{A;r} = e^{-\beta_r H_r}$ and check the validity of this assumption with our numerics.

Since the operator $T_{A;\theta}$ acts as the translation of the edge CFT, the partial rotation is expressed as the expectation values of translation operators within the edge CFT as

$$\mathcal{T}_{1}\left(\frac{2\pi}{n}\right) = \frac{\operatorname{Tr}\left[e^{iP_{ln}L}e^{-\frac{\xi_{l}}{v}H_{l}}\right]\operatorname{Tr}\left[e^{iP_{rn}L}e^{-\frac{\xi_{r}}{v}H_{r}}\right]}{\operatorname{Tr}\left[e^{-\frac{\xi_{l}}{v}H_{l}}\right]\operatorname{Tr}\left[e^{-\frac{\xi_{r}}{v}H_{r}}\right]}$$
$$= \frac{\chi_{1}\left(\frac{i\xi_{l}}{L} + \frac{1}{n}\right)\chi_{1}\left(\frac{i\xi_{r}}{L} - \frac{1}{n}\right)}{\chi_{1}\left(\frac{i\xi_{l}}{L}\right)\chi_{1}\left(\frac{i\xi_{r}}{L}\right)}, \tag{3}$$

where we introduced the velocity v, correlation length $\xi_l = v\beta_l$, $\xi_r = v\beta_r$, and the circumference of the cylinder L. P_l and P_r are translation operators on the left and right edge $P_l = -(1/v)H_l$, $P_r = (1/v)H_r$. $\chi_1(\tau)$ is the CFT character of the trivial sector with modular parameter τ . In our setup, where $L \ll \xi_l$, the characters for the left edge are approximated as

$$\chi_1\left(\frac{i\xi_l}{L}\right) \approx e^{\frac{2\pi\xi_{l^c}}{L}}, \quad \chi_1\left(\frac{i\xi_l}{L} + \frac{1}{n}\right) \approx e^{\frac{2\pi\xi_{l^c}}{L}} e^{-\frac{2\pi i c}{n}}. \quad (4)$$

Meanwhile, the edge CFT at the right edge cutting the system has high temperature $L \gg \xi_r$. These characters can

be approximately computed by performing proper modular S, T transformations as [30]

$$\chi_1\left(\frac{i\xi_r}{L}\right) = \sum_a S_{1,a} \chi_a\left(\frac{iL}{\xi_r}\right) \approx \frac{1}{\mathcal{D}} e^{\frac{2\pi L^c}{\xi_r^2}},\tag{5}$$

$$\begin{split} \chi_{1} \bigg(\frac{i\xi_{r}}{L} - \frac{1}{n} \bigg) &= \sum_{a} (ST^{n}S)_{1,a} \chi_{a} \bigg(\frac{iL}{n^{2}\xi_{r}} + \frac{1}{n} \bigg) \\ &\approx (ST^{n}S)_{1,1} e^{-\frac{2\pi i c}{n^{2}d}} e^{\frac{2\pi L c}{n^{2}\xi_{r}^{2d}}} \\ &= \frac{1}{\mathcal{D}^{2}} e^{-2\pi i (n + \frac{1}{n})\frac{c_{-}}{2d}} e^{\frac{2\pi L c}{n^{2}\xi_{r}^{2d}}} \sum_{a} d_{a}^{2}\theta_{a}^{n}, \end{split}$$
 (6)

where n is assumed to be small, satisfying $n^2 \ll L/\xi_r$. The sum is over the anyons a that label the conformal block of the edge CFT, and $\mathcal{D} = \sqrt{\sum_a d_a^2}$ is the total quantum dimension. By combining the above approximations of the characters, $\mathcal{T}_1(2\pi/n)$ in Eq. (3) is expressed as Eq. (2).

A similar computation can be performed when the ground state lives in a generic topological sector,

$$\mathcal{T}_a\left(\frac{2\pi}{n}\right) \propto e^{\frac{2\pi i}{n}h_a - 2\pi i (\frac{2}{n} + n)\frac{c_-}{24}} \times \zeta_{n,a},\tag{7}$$

where $\mathcal{T}_a(2\pi/n) \coloneqq \langle \Psi_a | T_{A;2\pi/n} | \Psi_a \rangle$, with $|\Psi_a\rangle$ being the ground state in the topological sector labeled by an anyon a. We defined the twisted higher central charge

$$\zeta_{n,a} \coloneqq \sum_{b} S_{ab} d_b \theta_b^n, \tag{8}$$

which is proportional to ζ_n when a = 1. The derivation of Eq. (7) is relegated to the Supplemental Material [21].

While the definition of the quantity (2) is akin to that of the momentum polarization in the large n limit [31,32], we emphasize that the partial rotation by the finite angle $\mathcal{T}_a(2\pi/n)$ extracts a completely different universal quantity from the momentum polarization. Indeed, the momentum polarization with $n \to \infty$ does not give the higher central charge, which is expressed as

$$\lim_{n \to \infty} \mathcal{T}_a \left(\frac{2\pi}{n} \right) \propto \exp \left[\frac{2\pi i}{n} \left(h_a - \frac{c_-}{24} - \frac{c_-}{24} \frac{L^2}{\xi_r^2} \right) \right]. \quad (9)$$

Remarkably, while Eq. (9) depends on the circumference L and the nonuniversal correlation length ξ_r , Eq. (2) solely gives a constant universal value as the combination of c_- and ζ_n . In the Supplemental Material [21], we describe how the behavior of the partial rotation interpolates between higher central charge and momentum polarization.

Numerical results.—We demonstrate the validity of the formula (2) for two examples: the Ising TQFT realized by the Kitaev honeycomb model and the U(1)₂ TQFT realized by the $\nu=1/2$ bosonic Laughlin state. Their $\zeta_{n,a}$ and

TABLE I. The phases of $\zeta_{n,a}$ and the partial rotation $\mathcal{T}_a(2\pi/n)$ for $n=1,\,2,\,3,\,4$ in each topological sector of Ising and $\mathrm{U}(1)_2$. We write 0 when the magnitude is vanishing.

	Sector a	$\zeta_{n,a}$	$T_a(2\pi/n)$
Ising	Trivial 1 σ	$e^{(2\pi i/16)}, e^{(2\pi i/16)}, e^{(6\pi i/16)}, e^{(4\pi i/16)}$ 1, 0, 1, 0	1, 1, $e^{(2\pi i/9)}$, $e^{(\pi i/16)}$ 1, 0, $e^{-(\pi i/9)}$, 0
$U(1)_2$	Trivial 1 Semion s	$e^{(2\pi i/8)},~0,~e^{-(2\pi i/8)},~1 \ e^{-(2\pi i/8)},~1,~e^{(2\pi i/8)},~0$	$e^{(13\pi i/9)}, e^{(13\pi i/8)}$ 1, 1, $e^{(\pi i/9)}, 0$

expected values of the partial rotation $\mathcal{T}_a(2\pi/n)$ are summarized in Table I. For some of the n's in a given topological sector, the magnitude of \mathcal{T}_1 vanishes. However, this could only occur when $\gcd(n, N_{\text{FS}}) \neq 1$, which therefore does not obscure the examination of whether the topological order has a gappable boundary.

The Kitaev honeycomb model is defined on a honeycomb lattice with a qubit on each vertex, with the Hamiltonian

$$H = J_{x} \sum_{\langle ij \rangle \in R \text{ edge}} X_{i}X_{j} + J_{y} \sum_{\langle ij \rangle \in B \text{ edge}} Y_{i}Y_{j}$$
$$+ J_{z} \sum_{\langle ij \rangle \in Y \text{ edge}} Z_{i}Z_{j} + \kappa \sum_{\langle ijk \rangle} X_{i}Y_{j}Z_{k}, \tag{10}$$

where the last term is introduced by turning on the magnetic field, which realizes the non-Abelian gapped phase [4]. The non-Abelian phase is known to host Ising TQFT with anyons 1, σ , and ψ with topological twists $\theta_1 = 1$, $\theta_\sigma = e^{2\pi i/16}$, and $\theta_\psi = -1$.

To compute partial rotation, we employ a cylinder geometry terminated with zigzag boundary condition on both ends as depicted in Fig. 2, and we act on the left half of the system with partial rotation.

The model is equivalent to a system of free Majorana fermions coupled to the \mathbb{Z}_2 gauge field by rewriting the qubits using Majorana fermion operators c, which act as dynamical free fermions, and b, which describes the \mathbb{Z}_2 gauge field. As demonstrated in the Supplemental Material [21], the partial rotation for the state on the cylinder lying in the trivial sector can be expressed as

$$\mathcal{T}_1\left(\frac{2\pi}{n}\right) \propto \text{Tr}\left(\frac{1+(-1)^F}{2}e^{-H_E}T_{A;\frac{2\pi}{n}}\right),$$
 (11)

where H_E is the entanglement Hamiltonian for the free fermion state in the A subsystem with the fixed flat \mathbb{Z}_2 gauge field, with the boundary condition in the y direction taken to be antiperiodic. The operator $[1 + (-1)^F]/2$ gives a projector onto the Hilbert space with even fermion parity. Following [31], one can further evaluate it from the entanglement spectrum of the free Majorana fermions,

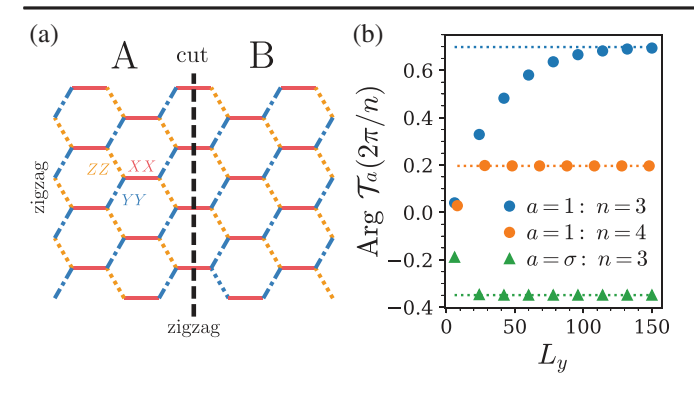


FIG. 2. (a) Geometry of the Kitaev model on a cylinder. Red, blue, and yellow lines correspond to X-, Y-, and Z-type Ising interactions, respectively. The lattice is periodic in the y direction and has the zigzag boundary condition in the x direction. (b) The partial rotations $\mathcal{T}_a(2\pi/n)$ evaluated in the Ising topological phase of the Kitaev model at n=3, 4. The σ sector at n=4 is not shown since it evaluates zero. We used $J_x=J_y=J_z=1$, $\kappa=0.1$ for computation.

$$\mathcal{T}_{1}\left(\frac{2\pi}{n}\right) \propto \prod_{m,k_{y}} \left[\frac{1 + e^{ik_{y}L_{y}/n}}{2} + \frac{1 - e^{ik_{y}L_{y}/n}}{2} \tanh\frac{\xi_{mk_{y}}}{2}\right] + \prod_{m,k_{y}} \left[\frac{1 - e^{ik_{y}L_{y}/n}}{2} + \frac{1 + e^{ik_{y}L_{y}/n}}{2} \tanh\frac{\xi_{mk_{y}}}{2}\right], \quad (12)$$

where ξ_{mk_y} is the entanglement spectrum for H_E , carried by a quasiparticle with momentum k_y in the y direction. Analogously, the partial rotation for the σ sector is expressed in terms of the entanglement Hamiltonian H_E^{σ} given by setting the periodic boundary condition in the y direction, $\mathcal{T}_{\sigma}(2\pi/n) \propto \text{Tr}(e^{-H_E^{\sigma}}T_{A;2\pi/n})$, which can also be computed from entanglement spectrum of H_E^{σ} .

We show the result of this evaluation for 1, σ sectors in Fig. 2. We see that $\operatorname{Arg}[\mathcal{T}_a(2\pi/n)]$ converges to predicted values. We only present for $n \geq 3$ and $|\mathcal{T}_a(2\pi/n)| > 0$. $\mathcal{T}_a(2\pi/n)$ is always real (no phase) for n=1 and 2 since the phase part exactly cancels.

The second example is the $\nu = 1/2$ bosonic Laughlin state, which realizes the U(1)₂ Chern-Simons theory. Its only nontrivial anyon is the semion s with $\theta_s = i$.

The model we study is a half filled lowest Landau level (LLL) of two-dimensional bosons with a contact interaction $V_0=1$ plus a small perturbation $\delta V_2=0.1$, where V_m are the Haldane pseudopotentials [33,34]. We consider an infinite cylinder geometry [Fig. 3(a)] and use infinite density matrix renormalization group calculations [35] to obtain the infinite matrix product state (iMPS) representation of the ground state $|\Psi\rangle$.

Compared to other numerical methods, the MPS representation is advantageous for evaluating the action of partial rotation. If rotation is a good symmetry, the Schmidt states $|\alpha\rangle_{A/B}$ across subsystems A and B have

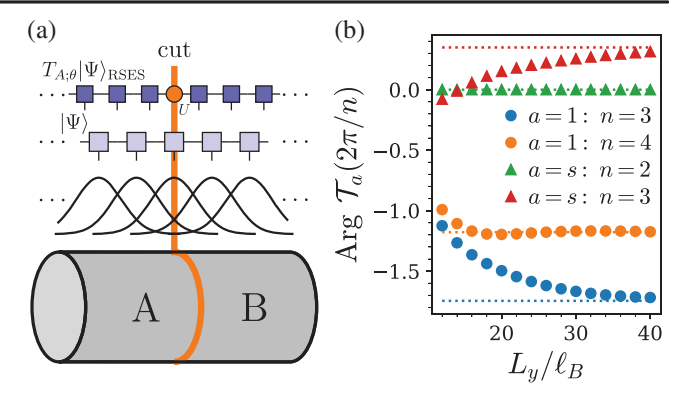


FIG. 3. (a) A schematic of the infinite cylinder geometry and the LLL orbital basis of the MPS. Partial rotation along a real-space cut can be accomplished by acting a unitary operator on the auxiliary bond of the MPS obtained by the RSES algorithm. (b) $\operatorname{Arg}\mathcal{T}_a(2\pi/n)$ of the $\nu=1/2$ bosonic Laughlin state extracted using Eq. (13). The dotted lines are the CFT predictions given in Table I.

definite momentum k_y^{α} along the circumference. Thus, the action of partial rotation can be evaluated by

$$\mathcal{T}_{a}(\theta) = \sum_{\alpha} \lambda_{\alpha}^{2} e^{ik_{y}^{\alpha} L_{y} \theta}, \tag{13}$$

where λ_{α} is the corresponding Schmidt value. We can easily obtain both k_{y}^{α} and λ_{α} from the momentum label $\bar{K}_{\bar{n}_{B};\alpha}$ and the Schmidt value $\lambda_{\bar{n}_{B};\alpha}$ of the auxiliary bond \bar{n}_{B} across subsystems A and B.

For the $\nu=1/2$ bosonic Laughlin state, we work in the Landau gauge and the corresponding LLL orbital basis. To accelerate the calculation and obtain the momentum label mentioned above, we incorporate both particle number $\hat{C}=\sum_n\hat{C}_n\equiv\sum_n(\hat{N}_n-\nu)$ and momentum $\hat{K}=\sum_n\hat{K}_n\equiv\sum_nn(\hat{N}_n-\nu)$ conservation, where \hat{N}_n is the number operator at site n. We find that $\mathcal{T}_a(2\pi/n)$ converges at bond dimension $\chi=3200$, cylinder circumference $L_{\nu}=40\ell_B$, and on site boson number cutoff $N_{\rm boson}=5$.

We note that there are a few technical complications in applying Eq. (13) to compute $\mathcal{T}_a(\theta)$, we will sketch here; readers can find more details in the Supplemental Material [21]. First, there are a few ambiguities in extracting the physical momentum k_y^α from the momentum label $\bar{K}_{\bar{n}_A;\alpha}$. For iMPS, there is an overall ambiguity of momentum labels on auxiliary bonds. The magnetic translation symmetry in quantum Hall systems further tangles the momentum label $\bar{K}_{\bar{n};\alpha} = \langle \sum_{n < \bar{n}} \hat{K}_n \rangle_\alpha$ with the charge label $\bar{C}_{\bar{n};\alpha} = \langle \sum_{n < \bar{n}} \hat{C}_n \rangle_\alpha$ [36]. These ambiguities can be fixed by matching the entanglement spectrum and the edge CFT spectrum as elaborated in the Supplemental Material [21].

Second, which topological sector subsystem A, B belongs to depends on the cut. The $\nu = 1/2$ bosonic

Laughlin state has a twofold ground state degeneracy, characterized by root configuration (pattern of zeros) [01] and [10] [37,38]. It turns out that cutting through the LLL orbital center that corresponds to the 0s (1s) bisects the system into two trivial sectors (semion) sectors. Finally, when we work in the LLL orbital basis, an auxiliary bond divides the system into two sets of LLL orbitals instead of two regions of physical space. This problem can be resolved using the real-space entanglement spectrum (RSES) algorithm developed in [36]. We note that many of the technicalities discussed here are not specific to the $\nu=1/2$ bosonic Laughlin state, but provide a general procedure for computing higher central charge of arbitrary wave function in the MPS form.

Finally, we present the result of $\mathcal{T}_a(2\pi/n)$ in both the trivial and the semion sectors. As shown in Fig. 3(b), $\mathcal{T}_a(2\pi/n)$ always converges to the expected phase as shown in Table I at sufficiently large L_v .

Discussion.—In this Letter, we characterize the higher central charges $\{\zeta_n\}$ in terms of the partial rotation evaluated on a wave function of the (2+1)D bosonic topological order and confirmed the prediction using the Kitaev honeycomb model and the $\nu=1/2$ bosonic Laughlin state. Partial rotation can be implemented easily in quantum computing architectures with cheap SWAP gates, such as Rydberg atom arrays, which opens up another avenue to studying topological order directly on a quantum computer. Together with topological entanglement entropy, partial rotation allows us to fully determine edge gappability of Abelian topological order.

It would be interesting to study applications of partial rotation to generic non-Abelian topological phases. Remarkably, even for non-Abelian phases, numerical results of $\{\mathcal{T}_1(2\pi/n)\}$ put a tight constraint on the possible low-energy spectrum of the bulk-boundary system. For instance, suppose that we observed $\{\mathcal{T}_1(2\pi/p_j)\}$ is a nontrivial phase for a set of distinct prime numbers $\{p_j\}$. One can see that this leaves us two possibilities: (1) the edge is ungappable, or (2) the edge is gappable, where $N_{\rm FS}$ must be divisible by $\prod_j p_j$. If the minimal $N_{\rm FS}$ required for a gappable edge is large and physically unrealistic, one can essentially determine that the boundary must be ungappable.

Notably, the lower bound $N_{\rm FS} \geq \prod_j p_j$ for a gappable edge implies the lower bound for the number of anyons r given by $r \geq r_0$, with r_0 the smallest integer satisfying $2^{2r_0/3+8}3^{2r_0/3} \geq \prod_j p_j$. This is derived from the fact that $N_{\rm FS}$ of the bosonic topological order with r distinct anyons has the upper bound $N_{\rm FS} \leq 2^{2r/3+8}3^{2r/3}$ [39]. It implies that the ground state on a torus must carry at least r_0 -fold degeneracy in order to realize a gappable edge. This argument is reminiscent of the Lieb-Schultz-Mattis-type theorems [40–42], which constrain the low-energy spectrum for a given input of the symmetry action on the ground state.

Also, it would be interesting to extract the higher Hall conductivity proposed in [43], which gives an obstruction to U(1) symmetry-preserving gapped boundary of the fermionic topological order with U(1) symmetry beyond electric Hall conductivity and c_- .

We thank Michael Zaletel, Roman Geiko, and Tianle Wang for helpful discussions. R. K. is supported by the JOI postdoctoral fellowship at the University of Maryland. T. W. is supported by the U.S. DOE, Office of Science, Office of Basic Energy Sciences, Materials Sciences and Engineering Division, under Award No. DE-AC02-05-CH11231, within the Van der Waals Heterostructures Program (KCWF16). T. S. is supported by a fellowship from the Masason foundation. R. M. is supported by the National Science Foundation under Grant No. DMR-1848336. S. R. is supported by the National Science Foundation under Grant No. DMR-2001181 and by a Simons Investigator Grant from the Simons Foundation (Grant No. 566116). This work is supported by the Gordon and Betty Moore Foundation through Grant No. GBMF8685 toward the Princeton theory program. This research used the Lawrencium computational cluster resource provided by the IT Division at the Lawrence Berkeley National Laboratory (Supported by the Director, Office of Science, Office of Basic Energy Sciences of the U.S. Department of Energy under Award No. DE-AC02-05CH11231).

- *ryok@umd.edu
- [1] X.-G. Wen, Quantum Field Theory of Many-Body Systems: From the Origin of Sound to an Origin of Light and Electrons (Oxford University Press, New York, 2004).
- [2] Y. Hatsugai, Phys. Rev. Lett. 71, 3697 (1993).
- [3] C. L. Kane and M. P. A. Fisher, Phys. Rev. B **55**, 15832 (1997).
- [4] A. Kitaev, Ann. Phys. (Amsterdam) 321, 2 (2006).
- [5] N. P. Mitchell, L. M. Nash, D. Hexner, A. M. Turner, and W. T. M. Irvine, Nat. Phys. 14, 380 (2018).
- [6] I. H. Kim, B. Shi, K. Kato, and V. V. Albert, Phys. Rev. Lett. 128, 176402 (2022).
- [7] I. H. Kim, B. Shi, K. Kato, and V. V. Albert, Phys. Rev. B 106, 075147 (2022).
- [8] Y. Zou, B. Shi, J. Sorce, I. T. Lim, and I. H. Kim, Phys. Rev. Lett. 129, 260402 (2022).
- [9] R. Fan, Phys. Rev. Lett. 129, 260403 (2022).
- [10] R. Fan, R. Sahay, and A. Vishwanath, Phys. Rev. Lett. **131**, 186301 (2023).
- [11] K. Shiozaki, H. Shapourian, K. Gomi, and S. Ryu, Phys. Rev. B 98, 035151 (2018).
- [12] H. Dehghani, Z.-P. Cian, M. Hafezi, and M. Barkeshli, Phys. Rev. B 103, 075102 (2021).
- [13] Z.-P. Cian, H. Dehghani, A. Elben, B. Vermersch, G. Zhu, M. Barkeshli, P. Zoller, and M. Hafezi, Phys. Rev. Lett. 126, 050501 (2021).
- [14] A. Kapustin and N. Saulina, Nucl. Phys. **B845**, 393 (2011).
- [15] M. Levin, Phys. Rev. X 3, 021009 (2013).

- [16] S.-H. Ng, A. Schopieray, and Y. Wang, Sel. Math. **25**, 53 (2019).
- [17] S.-H. Ng, E. C. Rowell, Y. Wang, and Q. Zhang, Adv. Math. 404, 108388 (2022).
- [18] J. Kaidi, Z. Komargodski, K. Ohmori, S. Seifnashri, and S.-H. Shao, SciPost Phys. **13**, 067 (2022).
- [19] A. Kitaev and J. Preskill, Phys. Rev. Lett. **96**, 110404 (2006).
- [20] M. Levin and X.-G. Wen, Phys. Rev. Lett. 96, 110405 (2006).
- [21] See Supplemental Material at http://link.aps.org/ supplemental/10.1103/PhysRevLett.132.016602 which includes Refs. [22–26] for determination of edge gappability, partial rotation in twisted sector, and details on numerical simulation.
- [22] V. Drinfeld, S. Gelaki, D. Nikshych, and V. Ostrik, arXiv: 0906.0620.
- [23] X.-G. Wen, Phys. Rev. Lett. 90, 016803 (2003).
- [24] S. D. Geraedts, C. Repellin, C. Wang, R. S. K. Mong, T. Senthil, and N. Regnault, Phys. Rev. B 96, 075148 (2017).
- [25] T. Soejima, D. E. Parker, N. Bultinck, J. Hauschild, and M. P. Zaletel, Phys. Rev. B 102, 205111 (2020).
- [26] N. Read, Phys. Rev. B 79, 045308 (2009).
- [27] X.-L. Qi, H. Katsura, and A. W. W. Ludwig, Phys. Rev. Lett. 108, 196402 (2012).
- [28] While the argument in [27] is valid for chiral (i.e., holomorphic) edge CFT, one can utilize the cut-and-glue approach for nonchiral edge CFT as well, as demonstrated in the Supplemental Material [21].

- [29] H. Li and F. D. M. Haldane, Phys. Rev. Lett. 101, 010504 (2008).
- [30] K. Shiozaki, H. Shapourian, and S. Ryu, Phys. Rev. B 95, 205139 (2017).
- [31] H.-H. Tu, Y. Zhang, and X.-L. Qi, Phys. Rev. B 88, 195412 (2013).
- [32] M. P. Zaletel, R. S. K. Mong, and F. Pollmann, Phys. Rev. Lett. 110, 236801 (2013).
- [33] E. H. Rezayi and F. D. M. Haldane, Phys. Rev. B 50, 17199 (1994).
- [34] B. I. Halperin, J. K. Jain, and N. R. Cooper, Fractional Quantum Hall States of Bosons: Properties and Prospects for Experimental Realization (World Scientific, Singapore, 2020), pp. 487–521.
- [35] M. P. Zaletel, R. S. K. Mong, F. Pollmann, and E. H. Rezayi, Phys. Rev. B 91, 045115 (2015).
- [36] M. P. Zaletel and R. S. K. Mong, Phys. Rev. B 86, 245305 (2012).
- [37] B. A. Bernevig and F. D. M. Haldane, Phys. Rev. Lett. 100, 246802 (2008).
- [38] X.-G. Wen and Z. Wang, Phys. Rev. B 78, 155109 (2008).
- [39] P. Bruillard, S.-H. Ng, E. Rowell, and Z. Wang, J. Am. Math. Soc. 29, 857 (2016).
- [40] E. Lieb, T. Schultz, and D. Mattis, Ann. Phys. (N.Y.) 16, 407 (1961).
- [41] M. Oshikawa, Phys. Rev. Lett. 84, 1535 (2000).
- [42] M. Hastings, Phys. Rev. B 69, 104431 (2004).
- [43] R. Kobayashi, Phys. Rev. Res. 4, 033137 (2022).